Imaging of Multiple Linear Cracks Using Impedance Data ⋆

Kurt Bryan, [1] Rachel Krieger, [2] Nic Trainor [3]

Abstract

This paper develops a fast, simple algorithm for locating one or more perfectly insulating, pair-wise disjoint, linear cracks in a homogeneous two-dimensional electrical conductor, using flux-potential boundary measurements. We also explore the issue of what types boundary inputs yield the most stable images.

Key words: inverse problem, cracks, impedance imaging
PACS:

1 Introduction

Impedance imaging has received a great deal of attention from the mathematical community in recent years, and in particular the development of fast, stable algorithms for specific subclasses of the general problem are of continuing interest. One such subclass of problems consists of imaging cracks in an otherwise homogeneous electrical conductor.

⋆ This work was partially supported by the National Science Foundation under an REU grant, DMS-0097804.
[1] Dept. of Mathematics, Rose-Hulman Institute of Technology, Terre Haute, IN
[2] Mathematics Dept., University of Michigan, Flint MI
[3] Dept. of Mathematics, Rutgers University, New Brunswick NJ

The problem was first considered in [9], in which the authors prove a uniqueness result for the problem. Specifically, they show that any perfectly insulating or conductive crack in a two-dimensional region with real-analytic background conductivity can be uniquely determined using measured boundary potentials (Dirichlet data) corresponding to two input current fluxes (Neumann data) of a certain form. They also show that in general, one input current flux may not suffice. The papers [1] and [10] show, independently, that two appropriate input-flux/boundary-potential pairs suffice to identify any finite collection of cracks. In [14] the authors propose a computational algorithm for recovering line-segment crack from boundary data, and consider the issue of which types of input current fluxes yield the most stable estimates. In [11] the algorithm is demonstrated to be effective on experimentally collected data. The algorithm was extended to the multiple crack case in [7]. See [8] for a more thorough review of the many theoretical and numerical results on the problem of crack identification.

Our purpose in this paper is to develop another approach to imaging cracks, one that is especially suitable for imaging multiple cracks in a bounded domain. The method is fast, accurate, and conceptually quite simple. It also has the advantage that, unlike most prior approaches, one need not guess at the number of cracks present, but rather the method gives quantitative information about the number of cracks contained in the region (the issue of estimating the number of cracks present has also been consider in [3]). Our method has many similarities to those developed to image small inhomogeneities in a domain with known reference conductivity; see, for example, [2]. We also address the issue of which types of input fluxes provide optimal sensitivity and resolution for imaging cracks.

Section 2 below contains a careful statement of the forward problem. In Section 3 we state a technical result, Lemma 1, upon which our inversion procedure is based. In Section 4 we explain the inversion algorithm, provide many computational examples, and discuss what types of input flux provide maximum resolution and stability. The proof of Lemma 1 is contained in Section 5.

2 The Forward Problem

Let Ω be a bounded region in $\mathbb{R}^2$ with suitably smooth boundary $\partial\Omega$. We suppose that Ω contains a collection $\Sigma = \cup_{j=1}^{n}\sigma_j$ of cracks σ_j. Each crack is assumed to be a line segment, with the cracks pairwise disjoint and a non-zero distance from $\partial\Omega$. Let $u(x, y)$ denote the electric potential induced in $\Omega \setminus \Sigma$ by an input current flux g applied to $\partial\Omega$, where $\int_{\partial\Omega} g\, ds = 0$. After suitable rescaling we assume that u satisfies

$$\triangle u = 0 \text{ in } \Omega \setminus \Sigma \tag{1}$$

$$\frac{\partial u}{\partial \mathbf{n}} = g \text{ on } \partial\Omega \tag{2}$$

$$\frac{\partial u}{\partial \mathbf{n}} = 0 \text{ on } \Sigma \tag{3}$$

where $\mathbf{n}$ is an outward unit normal vector field on $\partial\Omega$ or a consistently oriented unit normal on each crack σ_j, as appropriate. Equation (3) models the cracks as perfectly insulating. The boundary value problem (1)-(3) possesses a unique solution in $H^1(\Omega \setminus \Sigma)$ for a wide class of input fluxes, e.g., $g \in H^{-1/2}(\partial\Omega)$, provided we add the normalization $\int_{\partial\Omega} u\, ds = 0$.

The solution u is smooth away from the crack tips, but in general has a jump discontinuity across each crack. Let us denote one side of each crack as the "+" side, into which $\mathbf{n}$ points, and the other as the "−" side. Let u^+ denote the limiting value of u from the plus side of a crack, u^- the limiting value from the minus side, and define $[u] = u^+ - u^-$. Standard elliptic regularity theory shows that $[u]$ is continuous (indeed, smooth) along any given crack and tapers to zero at the crack endpoints, typically with square root singularities at the crack tips.

The inverse problem of interest is to identify Σ from one or more pairs of Cauchy data $(g, u|_{\partial\Omega})$. A number of identification and stability results have been obtained for this problem. In particular we note that two input current fluxes (of a specific form) and induced potentials serve to uniquely determine Σ, even when the cracks are not line segments; see [1] or [10].

In what follows we use z_j^*, $j = 1$ to n, to denote the center of each crack and θ_j for the angle of the jth crack with respect to the horizontal axis. Our results for the inverse problem are based on an asymptotic expansion involving the lengths of the cracks, and so we assume that the jth crack has length ϵL_j for some constant L_j, where $\epsilon > 0$ is used as the common length scale for the cracks.

3 Asymptotic Representation of the Forward Solution

Let $v(x)$ (where $x = (x_1, x_2) \in \mathbb{R}^2$) denote a harmonic function on Ω with suitably smooth boundary data. A straightforward application of the divergence theorem shows that

$$RG(v) := \int_{\partial\Omega} \left(u \frac{\partial v}{\partial \mathbf{n}} - v \frac{\partial u}{\partial \mathbf{n}} \right) ds = \sum_{j=1}^{n} \int_{\sigma_j} \frac{\partial v}{\partial \mathbf{n}} [u]\, ds. \tag{4}$$

The functional $RG(v)$ is sometimes called the "reciprocity gap" functional (see [5]), and has been used extensively for reconstructing information about a single crack in Ω, through judicious choice of test functions v. Note that $RG(v)$ is computable from a Cauchy data pair. If no cracks are present, $RG(v) = 0$ for any harmonic test function v.

If we have n cracks σ_j with centers z_j^* contained in Ω, normals $\mathbf{n}_j$, and lengths ϵL_j, $j = 1$ to n, then (since v is smooth in Ω) the Mean Value Theorem yields

$$\frac{\partial v}{\partial \mathbf{n}}(x) = \frac{\partial v}{\partial \mathbf{n}}(z_j^*) + E_j(x - z_j^*) \tag{5}$$

on each crack σ_j, where $E_j(x - z_j^*) \leq C|x - z_j^*|$ for some constant C. The constant C can be taken to be independent of the cracks provided all cracks lie in some compact subset of Ω (which is the case for ϵ sufficiently small). From equations (4) and (5) we find that

$$RG(v) = \sum_{j=1}^{n} J_j \frac{\partial v}{\partial \mathbf{n}}(z_j^*) + \sum_{j=1}^{n} \int_{\sigma_j} E_j(x - z_j^*)[u](x)\, ds. \tag{6}$$

where $J_j = \int_{\sigma_j} [u]\, ds$.

In the Section 5 we prove the following Lemma.

Lemma 1 *Let u denote the solution to the boundary value problem (1)-(3) for line segment cracks σ_j, $j = 1$ to $j = n$, with centers z_j^*, normal vectors $\mathbf{n}_j$ and lengths ϵL_j. Let $J_j = \int_{\sigma_j} [u]\, ds$. Then*

$$J_j = \frac{\pi}{4}\epsilon^2 \frac{\partial u_0}{\partial \mathbf{n}_j}(z_j^*) L_j^2 + O(\epsilon^3)$$

for all ϵ in some neighborhood of zero, where u_0 denotes a harmonic function on Ω with Neumann data g and $O(\epsilon^3)$ denotes a quantity with $|O(\epsilon^3)| \leq C\epsilon^3$, where C is independent of the L_j.

Now note that (since E_j is continuous)

$$\left| \int_{\sigma_j} E_j(x - z_j^*)[u](x)\, ds \right| = |E_j(x^* - z_j^*)| \left| \int_{\sigma_j} [u](x)\, ds \right| \leq C\epsilon L_j |J_j|$$

for some $x^* \in \sigma_j$, and so from Lemma 1 we have

$$\left| \int_{\sigma_j} E_j(x - z_j^*)[u](x)\, ds \right| = O(\epsilon^3).$$

which with equation (6) yields an asymptotic relation in ϵ for $RG(v)$ in terms of the crack parameters:

Theorem 2 *Let u denote the solution to the boundary value problem (1)-(3) for line segment cracks σ_j, $j = 1$ to $j = n$, with centers z_j^*, normal vectors $\mathbf{n}_j$ and lengths ϵL_j. Let $J_j = \int_{\sigma_j}[u]\,ds$. Then*

$$RG(v) = \sum_{j=1}^{n} J_j \frac{\partial v}{\partial \mathbf{n}_j}(z_j^*) + O(\epsilon^3)$$

where $O(\epsilon^3)$ denotes a quantity with $|O(\epsilon^3)| \leq C\epsilon^3$, where C is independent of the L_j.

Note that by Lemma 1 the leading terms in $RG(v)$ which involve J_j will be $O(\epsilon^2)$. The core of our reconstruction procedure consists in deducing z_j^*, $\mathbf{n}_j$, and J_j from knowledge of $RG(v)$ (after dropping the $O(\epsilon^3)$ terms) for a certain class of test functions v. The value of z_j^* gives us the center of σ_j, while knowledge of $\mathbf{n}_j$ specifies the angle. Finally, we can use Lemma 1 to approximate the length of each crack from J_j, provided the cracks are sufficiently short.

4 Reconstruction of Cracks

In this section we will examine the use of Theorem 2 and Lemma 1 for the estimation of one or more cracks from one or more pairs of Cauchy data on $\partial\Omega$, as well as the types of input fluxes that will yield the most stable estimates. We begin by showing how to recover a single crack, then examine optimal input fluxes for stable imaging, and finally the recovery of multiple cracks. We also provide a quantitative method for estimating the number of cracks actually present.

For solving the forward problem (to generate test data for use in our inversions) we convert the PDE (1)-(3) into a system of integral equations supported on $\partial\Omega$ and Σ, which is then solved using Nyström's method. The solutions are accurate to at least 4 significant figures, based on comparison to closed form solutions.

Let us consider complex-valued test functions of the form $v(x) = e^{\eta(x_1+ix_2)}$ where $\eta \in \mathbb{C}$; the function v is harmonic for any choice of η. Inserting this test function into $RG(v)$ and dropping the $O(\epsilon^3)$ terms in Theorem 2 yields

$$RG(v) \approx \sum_{j=1}^{n} J_j \eta e^{\eta z_j^*}(n_1^j + in_2^j)$$

$$= i\eta \sum_{j=1}^{n} J_j e^{\eta z_j^*} e^{i\theta_j} \tag{7}$$

where $\mathbf{n} =< n_1^j, n_2^j >$ on the jth crack, and $n_1^j + i n_2^j = e^{i(\theta_j + \pi/2)} = i e^{i\theta_j}$.

We will consider $RG(v)$ as a function of η, and in fact define a function $\phi(\eta) = -iRG(\eta)/\eta$ so that we have

$$\phi(\eta) = \sum_{j=1}^{n} A_j e^{\eta z_j^*} \tag{8}$$

where $A_j = J_j e^{i\theta_j}$. Note that we can compute $\phi(\eta)$ for any complex number η; our goal is to use $\phi(\eta)$ to recover the z_j^* and A_j (hence J_j and θ_j). From this we can use Lemma 1 to estimate the length of each crack.

It is important to note that we can easily compute the derivatives of $\phi(\eta)$ with respect to η to any order, as

$$\phi^{(k)}(\eta) = -i \frac{d^k}{d\eta^k} \left(\frac{RG(\eta)}{\eta} \right)$$

which does NOT involve differentiating the boundary data, but merely the test functions involved in computing $RG(\eta)$.

4.1 Single Crack Reconstruction

Consider a single crack with center z^*, angle θ, length L, for which equation (8) becomes

$$\phi(\eta) = A e^{\eta z^*}. \tag{9}$$

For any given η_0 we can recover z^* from $\phi'(\eta_0)/\phi(\eta_0) = z^*$; we can then find A as $A = \phi(\eta_0) e^{-\eta_0 z^*}$, from which we find $\theta = \arg(A)$ and (via Lemma 1)

$$L \approx 2\sqrt{\frac{|A|}{\pi |\nabla u_0(z^*) \cdot \mathbf{n}|}} \tag{10}$$

(note that $\mathbf{n}$ is known once we know θ). The entire computation requires the evaluation of just two integrals over $\partial\Omega$.

4.1.1 Example 1: Single Crack Reconstruction; Choice of η_0

For this example we take Ω to be the unit disk in $\mathbb{R}^2$ and the flux on $\partial\Omega$ to be $g(t) = \sin(t)$, with $\partial\Omega$ parameterized as $(\cos(t), \sin(t))$, $0 \leq t < 2\pi$. The function u is computed at 50 equi-spaced points on the boundary of the disk. The corresponding harmonic function is $u_0(x) = x_2$. We consider a single crack σ with center $(0.432, 0.472)$, of length 0.3 at an angle of 0.5 radians with respect to horizontal. In the reconstruction procedure outlined above we have a choice for the value of η_0. The table below shows the reconstructed crack parameters for several choices of η_0, all of which are quite accurate:

η_0	z^*	L	θ
0.5	$(0.433, 0.474)$	0.286	0.499
1.0	$(0.435, 0.477)$	0.286	0.498
$1.0 + i$	$(0.438, 0.478)$	0.287	0.497
$-1.0 - i$	$(0.438, 0.461)$	0.288	0.501

However, it is worth noting that the choice of η_0 does in fact have some bearing on the stability of the computation, especially in the presence of noise. In general one expects that the boundary measurements of u on $\partial\Omega$ nearest the crack contain the "most" information, and so it should be expected that a choice of η_0 which weights this portion of the Dirichlet data for u more heavily in equation (7) will result in a more stable estimate. As an example, consider a crack with center z^*. Let us choose η_0 of some specified magnitude B so that the test function $v(x_1, x_2) = e^{\eta(x_1+ix_2)}$ in equation (7) attains its maximum magnitude on $\partial\Omega$ at that point on $\partial\Omega$ closest to z^*. If Ω is the unit disk then a simple computation shows that the optimal choice is $\eta_0 = \frac{B}{|z^*|}\bar{z^*}$ (while $\eta_0 = -\frac{B}{|z^*|}\bar{z^*}$ is the worst). This is illustrated by the data in the table below, which uses the same crack as above but in which normally distributed random noise has been to the potential data, with standard deviation equal to 10 percent of the maximum value of $u - u_0$ (the relevant "signal strength") on the boundary of the disk—a relatively large amount of noise for impedance imaging. In this case, since $z^* = 0.432 + 0.472i$, we expect (from the 6 choices for η_0 below) that $\eta_0 = 1 - i$ will give the best results (since $1 - i$ is most

closely a multiple of $\bar{z^*}$), while $\eta_0 = -1 + i$ the worst, as is in fact the case:

η_0	z^*	L	θ
0.5	$(0.446, 0.453)$	0.290	0.503
1.0	$(0.442, 0.430)$	0.290	0.520
$1.0 + i$	$(0.504, 0.390)$	0.278	0.525
$-1.0 - i$	$(0.408, 0.495)$	0.287	0.496
$1.0 - i$	$(0.413, 0.438)$	0.294	0.499
$-1.0 + i$	$(0.379, 0.512)$	0.284	0.553

Of course in reality we don't know z^* a priori, but as soon as we have an estimate of z^* based on a suboptimal choice for η_0, we can use the estimate to choose a new η_0 and compute a refined estimate of the crack parameters.

4.2 Optimal Input Flux

Equations (10) and (9) make it clear that the magnitude of the jump integral $J = \int_\sigma [u]\, ds$, and in particular the quantity $\nabla u_0(z^*) \cdot \mathbf{n}$ determines one's ability to detect and image cracks—for a single crack, the magnitude of $\nabla u_0(z^*) \cdot \mathbf{n}$ should be as large as possible, for given constraints on the input current g. In this subsection we make a brief examination of what types of input currents are optimal for finding a single crack (the results are also applicable to multiple cracks), especially in light of Lemma 1. Indeed, it is clear from Lemma 1 that we should choose a flux g which makes $\nabla u_0(z^*)$ parallel to $\mathbf{n}$ on a single crack σ. Of course, if the crack σ is unknown this is impossible—we envision rather an iterative scheme, in which partial knowledge of σ is used to design a flux g which gives more stable images (similar to the scheme used in [7]). We illustrate such a procedure in examples below.

To avoid confusion in what follows we will use the notation $\mathbf{n}^\sigma$ to denote the normal on the crack and simply $\mathbf{n}$ to refer to a unit outward normal on $\partial\Omega$.

Of central concern is the class of functions in which the flux g is allowed to lie. We consider two cases: $g \in L^2(\partial\Omega)$ and the case in which g consists of the sum of an $L^1(\partial\Omega)$ function and a finite number of delta functions. The latter choice allows a wider range of physically reasonable fluxes.

Let $N(x, y)$ denote the Neumann kernel for the boundary value problem $\triangle u_0 = 0$ on Ω with $\frac{\partial u_0}{\partial \mathbf{n}} = g$ on $\partial\Omega$, so that $N(x, y)$ satisfies

$$\begin{aligned}
\triangle_y N(x,y) &= \delta_x, \quad y \in \Omega \\
\frac{\partial N}{\partial \mathbf{n_y}}(x,y) &= \frac{1}{|\partial\Omega|}, \quad y \in \partial\Omega \\
\int_{\partial\Omega} N(x,y)\, ds_y &= 0
\end{aligned}$$

for each $x \in \Omega$, where $\triangle_y$ is the Laplacian in the y variable. (Note that $N(x,y) = \Gamma(x,y) + N_0(x,y)$, where $\Gamma(x,y) = \frac{1}{2\pi}\ln|x-y|$ and N_0 is smooth). For $x \in \Omega$ the harmonic function u_0 on Ω with Neumann data $\frac{\partial u_0}{\partial \mathbf{n}} = g$ can be expressed

$$u_0(x) = -\int_{\partial\Omega} N(x,y) g(y)\, ds_y.$$

We may differentiate under the integral to deduce that

$$\frac{\partial u_0}{\partial \mathbf{n}^\sigma}(z^*) = -\int_{\partial\Omega} \frac{\partial N}{\partial \mathbf{n}_x^\sigma}(z^*, y) g(y)\, ds_y$$

where $\frac{\partial N}{\mathbf{n}_x^\sigma} = \nabla_x N \cdot \mathbf{n}^\sigma$. We seek to maximize (or minimize) the quantity $\frac{\partial u_0}{\partial \mathbf{n}^\sigma}(z^*)$ as a functional of g, subject to constraints which depend upon the function space in which g lies.

For the case $g \in L^2(\partial\Omega)$ it is natural to impose $\int_{\partial\Omega} g^2\, ds \leq M$ for some constant M, which we take to be 1. To find the optimal flux g we thus obtain a straightforward and well-posed problem in the calculus of variations,

$$\max_{g \in L^2(\partial\Omega)} -\int_{\partial\Omega} \frac{\partial N}{\partial \mathbf{n}_x^\sigma}(z^*, y) g(y) ds_y \tag{11}$$

subject to constraints

$$\int_{\partial\Omega} g(y) ds_y = 0 \tag{12}$$

$$\int_{\partial\Omega} g^2(y) ds_y = 1. \tag{13}$$

A standard argument shows that the optimal $g \in L^2(\partial\Omega)$ is of the form

$$g(y) = \frac{1}{2\lambda_2}\left(\frac{\partial N}{\partial \mathbf{n}_x^\sigma}(z^*, y) + \lambda_1\right) \tag{14}$$

where $\lambda_1 = -\int_{\partial\Omega} \frac{\partial N}{\partial \mathbf{n}_x^\sigma}(z^*, y)\, ds_y = 0$ and

$$\lambda_2 = \pm\frac{1}{2}\left(\int\limits_{\partial\Omega}\left(\frac{\partial N}{\partial \mathbf{n}_x^\sigma}(z^*, y)\right)^2 ds_y\right)^{1/2}$$

(either the plus or minus sign can be taken). The function g specified by equation (14) has a simple physical interpretation, namely, $g = \pm\frac{v}{2\lambda_2}$ on $\partial\Omega$ where v satisfies the boundary value problem

$$\begin{aligned} \triangle v &= \delta_{z^*}^{\mathbf{n}^\sigma} \text{ in } \Omega \\ \frac{\partial v}{\partial \mathbf{n}} &= 0 \text{ on } \partial\Omega \\ \int\limits_{\partial\Omega} v(y)\, ds_y &= 0 \end{aligned}$$

where $\delta_{z^*}^{\mathbf{n}^\sigma}$ denotes a dipole source at z^* with orientation in the direction $\mathbf{n}^\sigma$.

Now let us consider the case in which the input flux g may consist of the sum of an $L^1(\partial\Omega)$ function and a finite number of delta functions (point masses) on $\partial\Omega$; we use G to denote the set of all such input fluxes. Such a g is of the form

$$g(y) = g_0(y) + \sum_{j=1}^{p} c_j \delta_{y_j}(y)$$

where $g_0 \in L^1(\partial\Omega)$. The analogue of (11)-(13) is

$$\max_{g\in G} -\int\limits_{\partial\Omega} \frac{\partial N}{\partial \mathbf{n}_x^\sigma}(z^*, y) g(y) ds_y \tag{15}$$

subject to constraints

$$\int\limits_{\partial\Omega} g_0(y) ds_y + \sum_{j=1}^{p} c_j = 0 \tag{16}$$

$$\int\limits_{\partial\Omega} |g_0(y)| ds_y + \sum_{j=1}^{p} |c_j| = 1 \tag{17}$$

where this last constraint is the natural way to limit the total input current.

For notational simplicity, set $\psi(y) = -\frac{\partial N}{\partial \mathbf{n}_x^\sigma}(z^*, y))$. Let $M = \max_{y\in\partial\Omega} \psi(y)$ and suppose that this maximum occurs at $y = y_M$; similarly, let $m = \min_{y\in\partial\Omega} \psi(y)$ with the minimum at $y = y_m$; whether y_m or y_M is unique is irrelevant.

Claim: The optimal g is given by $g = \frac{1}{2}\delta_{y_M} - \frac{1}{2}\delta_{y_m}$.

To see this, let $g_0^+(y) = \max(g_0(y), 0)$, $g_0^-(y) = \min(g_0(y), 0)$, with $r_1 = \int_{\partial\Omega} g_0^+ \, ds$, $r_2 = -\int_{\partial\Omega} g_0^- \, ds$. Also set $c_j^+ = \max(c_j, 0)$, $c_j^- = \min(c_j, 0)$ with $r_3 = \sum_{j=1}^p c_j^+$ and $r_4 = \sum_{j=1}^p c_j^-$. Note that condition (16) forces $r_1 - r_2 + r_3 - r_4 = 0$ and (17) forces $r_1 + r_2 + r_3 + r_4 = 1$, from which we conclude that $r_1 + r_3 = r_2 + r_4 = 1/2$. It is also immediate that

$$\begin{aligned}
\int_{\partial\Omega} \psi(y) g_0^+(y) \, ds_y &\leq r_1 M = r_1 \psi(y_M), \\
\int_{\partial\Omega} \psi(y) g_0^-(y) \, ds_y &\leq -r_2 m = r_2 \psi(y_m), \\
\sum_j c_j^+ \psi(y_j) &\leq r_3 M = r_3 \psi(y_M) \\
\sum_j c_j^- \psi(y_j) &\leq r_4 m = r_4 \psi(y_m).
\end{aligned}$$

Adding the above inequalities and using $r_1 + r_3 = r_2 + r_4 = 1/2$ yields

$$\int_{\partial\Omega} \psi(y) g(y) \, ds_y \leq \frac{1}{2}\phi(y_M) - \frac{1}{2}\phi(y_m)$$

which proves the claim.

As a simple illustration, let σ be a crack in the unit disk with center at $(0.1, 0.6)$, length 0.3, at angle $\pi/4$. Let the boundary of the disk be parameterized as $(\cos(t), \sin(t))$, $0 \leq t < 2\pi$. We consider three different fluxes, all scaled so that $\int_{\partial\Omega} |g(t)| \, dt = 1$. Using the input flux $g(t) = \sin(t)/4$ induces a jump $J = 0.01288$ over σ. The optimal $L^2(\partial\Omega)$ input flux induces a jump $J = 0.02655$, and the optimal delta function flux $g(t) = \frac{1}{2}\delta_{y_M} - \frac{1}{2}\delta_{y_m}$ (with $y_M \approx (\cos(0.8), \sin(0.8)), y_m \approx (\cos(1.46), \sin(1.46))$) induces a jump $J = 0.032$.

4.3 Generalization to Multiple Cracks

An algorithm for locating n line segment cracks was given in [4] by Bryan and Vogelius, using a Newton-like method. However, the algorithm relied on solving many boundary value problems at each iteration. Moreover, the algorithm needed multiple input fluxes (one for each tentative crack) and also required one to make an a priori guess at the number of cracks present, with a somewhat ad hoc procedure for adaptively estimating the number of cracks

(some work has been done on more quantitative procedures for estimating the number of cracks present; see [3]).

We consider an algorithm for multiple crack reconstructions based on equation (8), which can use only a single input flux, although multiple input fluxes are easily accommodated. We also show how one can quantitatively, to good approximation, determine precisely how many cracks are present inside Ω. No forward solves of the boundary value problem are required.

As previously noted, for a given input flux g and measured Dirichlet data we can evaluate $\phi(\eta)$ and the derivatives $\phi^{(k)}(\eta)$ of any order with relative stability. We will exploit this fact to estimate the (finite) number of terms present in the sum on the right in equation (8), and then to identity the crack centers z_j^* and the coefficients A_j. We then use equation (10) to determine the length of each crack, as well as the crack angles.

The identification of a sum of exponentials like that in equation (8) often occurs in signal processing and filter design. A classical procedure for identifying the z_j^* and A_j is given by *Prony's Method*, in which one evaluates $\phi(\eta)$ at integers k (or any points $\eta = z_1 + kz_2$ for complex numbers z_1, z_2). Many variations and improved versions have been given; see, for example, [12].

We instead exploit our ability to stably compute the derivatives of $\phi(\eta)$. Note that the function $\phi(\eta)$ defined by equation (8) satisfies the ordinary differential equation

$$\phi^{(n)}(\eta) + c_{n-1}\phi^{(n-1)}(\eta) + \cdots + c_1\phi'(\eta) + c_0\phi(\eta) = 0 \tag{18}$$

where the c_j are defined by the characteristic polynomial for the ODE (18)

$$p(x) = \prod_{j=1}^{n}(x - z_j^*) = x^n + \sum_{j=0}^{n-1} c_j x^j. \tag{19}$$

We can identify the coefficients c_j as follows: Choose points $\eta_1, \ldots, \eta_N$ with $N \geq n$ and evaluate $\phi^{(j)}(\eta_k)$ for $0 \leq j \leq n$, $1 \leq k \leq N$. From equation (18) we then obtain a (possibly over-determined) system of N linear equations in n unknowns, the c_j for $0 \leq j \leq n-1$. From this information we can recover the c_j, provided the η_k are chosen appropriately. We can then recover the z_j^* by finding the roots of $p(x)$. Finally, we obtain the coefficients A_j by solving the (possibly over-determined) linear system

$$\sum_{j=1}^{n} A_j e^{\eta_k z_j^*} = \tilde{\phi}(\eta_k) \tag{20}$$

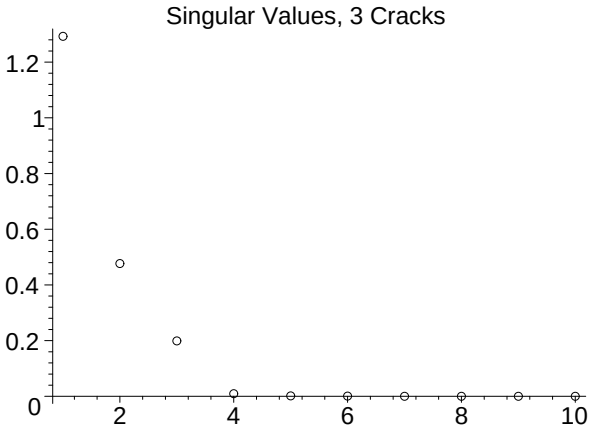

Fig. 1. First 10 singular values of $\mathbf{M}$, 3 cracks.

$1 \leq k \leq N$, where $\tilde{\phi}$ denotes the value of ϕ computed from the measured boundary data. We then use equation (10) (with $A = A_j$) to compute the length of each crack, and take $\theta_j = \arg(A_j)$ to estimate the crack angle.

We can actually estimate the number of cracks present as follows. Let $n_1 \geq n$ be a bound on the number of cracks in Ω. If we take $N \geq n_1$ and use $\eta = \eta_k$, $1 \leq k \leq N$, the system of linear equations obtained from equation (18) can be expressed $\mathbf{Mc} = \mathbf{b}$ where $\mathbf{c} = (c_0, c_1, \ldots, c_{n_1-1})^T$, $b_k = -\phi^{(n_1)}(\eta_k)$, and $\mathbf{M}$ is the N by n_1 matrix

$$M_{k,j+1} = \phi^{(j)}(\eta_k) \tag{21}$$

with $0 \leq j \leq n_1 - 1$, $1 \leq k \leq N$. If in fact only $n \leq n_1$ cracks are present then it's easy to see that $\mathbf{M}$ will have rank n (up to approximation error, assuming noiseless data, of course).

4.3.1 Example 2: Multiple Crack Reconstruction from a Single Flux

As an illustration of how one can determine number of cracks present and reconstruct them via the above procedure, consider the following example in which Ω is the unit disk, the input flux is $g(t) = \sin(t)$ with $0 \leq t < 2\pi$ as above. We solve the boundary value problem (1)-(3) with 3 cracks: crack 1 has center $(-0.4, -0.4)$, length 0.2, angle 0; crack 2 has center $(-0.06, 0.56)$, length 0.3, angle 0.4; crack 3 has center $(0.65, -0.03)$, length 0.3, angle -0.2 radians. We take upper bound $n_1 = 9$, then compute $\tilde{\phi}^{(j)}(\eta)$ for $j \leq 9$ and for 36 points of the form $\eta = (j - 3.5) + (k - 3.5)i$, $1 \leq j, k \leq 6$, and form the matrix $\mathbf{M}$.

The plot below shows the magnitude of the singular values of the matrix $\mathbf{M}$ up to the 10th singular value. Note that only the first 3 singular values are (significantly) non-zero. More generally, the number of cracks can be estimated

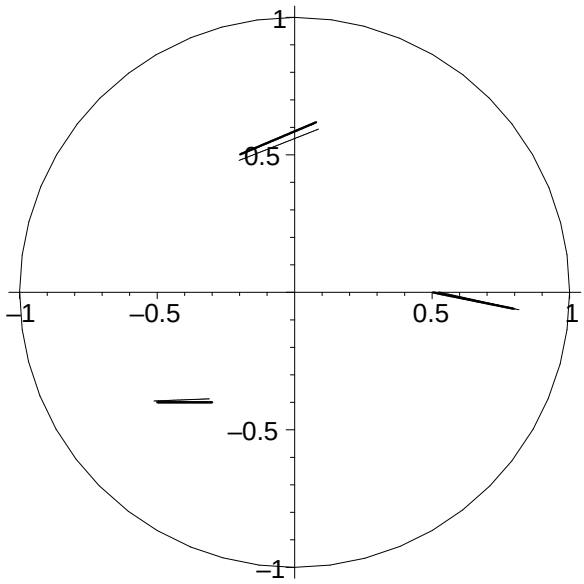

Fig. 2. True and estimated cracks.

by simply thresholding the singular values; in what follows we estimate the number of cracks by counting the number of singular values which exceed some fraction (in our case we use five percent) of the first (largest) singular value.

Based on the singular values of $\mathbf{M}$ we deduce that only 3 cracks are present. We then solve the system $\mathbf{Mc} = \mathbf{b}$ with $n_1 = 3$ (so that $\mathbf{M}$ has dimension 25×3) in a least-square sense. In this case we obtain $c_0 \approx -0.1511 + 0.1386i$, $c_1 \approx -0.0810 - 0.0822i$, $c_2 \approx -0.1981 - 0.1159i$. The polynomial $p(x) = x^3 + c_2x^2 + c_1x + c_0$ has roots $z_1^* \approx -0.411 - 0.388i$, $z_2^* \approx -0.063 + 0.535i$, $z_3^* \approx 0.673 - 0.031i$. All of these are quite close to the correct values.

We then solve the over-determined system (20) in a least-square sense to find $A_1 \approx 0.0322 + 0.0018i$, $A_2 \approx 0.066 + 0.0249i$, and $A_3 \approx 0.0663 - 0.0149i$. From equation (10) we then obtain $\theta_1 \approx 0.055$, $\theta_2 \approx 0.36$, $\theta_3 \approx -0.22$, and $L_1 \approx 0.203, L_2 \approx 0.310, L_3 \approx 0.298$. The lengths are very close to the correct values and the angles, though not quite as close, are reasonably good. Below is a picture of the original (solid line) and estimated (lighter dashed lines) cracks, based on only a single input flux:

We should note that if one mis-estimates the number of cracks—in particular, over-estimates—the algorithm still performs well. In the above example, if we attempt to recover four or more cracks from the data we obtain essentially the same estimate as above, but with very short additional cracks (almost invisible in the figure, which we omit). Underestimating the number of cracks results in a more objectionable "averaging" of the cracks. It thus seems appropriate to error on the side of overestimating the number of cracks.

4.3.2 Example 3: Multiple Crack Reconstruction with Multiple Input Fluxes; Noisy Data

The algorithm outlined above is easily adapted to multiple input fluxes. Specifically, let p different input fluxes $g_1, \ldots, g_p$ be applied, and let ϕ_m, $1 \leq m \leq p$, denote the functions defined by equations (7)-(8), using, of course, g_m and the corresponding Dirichlet data. Since the z_j^* do not depend on the input flux, we see that each of the ϕ_m independently satisfy the differential equation (18) (merely with different constants A_j). Similar to the remarks preceding equation (21) let n_1 be an upper bound on the number of cracks present, and let $\mathbf{M}^m$ denote the $N \times n_1$ matrix defined by $M^m_{k,j+1} = \phi_m^{(j)}(w_k)$ so that $\mathbf{M}^m\mathbf{c} = \mathbf{b}^m$, where $\mathbf{b}^m$ is the vector with components $b_k = -\phi_m^{(n_1)}(\eta_k)$. Let

$$\mathbf{M} = [(\mathbf{M}^1)^T|(\mathbf{M}^2)^T|\cdots(\mathbf{M}^p)^T]^T$$

denote the matrix which governs the "stacked" system $\mathbf{Mc} = \mathbf{b}$ with $\mathbf{b} = [(\mathbf{b}^1)^T|(\mathbf{b}^2)^T|\cdots(\mathbf{b}^p)^T]^T$. If there are truly n cracks present then as before the matrix $\mathbf{M}$ should (up to approximation and data error) have rank n. As before, we can solve for the coefficients $c_0, \ldots, c_{n-1}$ and find the roots z_j^* to equation (19) to locate the crack centers.

After locating the crack centers we can then use any of the p systems defined by equation (20) to recover the A_j (which differ for each input flux), and then use equation (10) to estimate the length of the jth crack, and $\arg(A_j)$ to estimate the crack angle. In estimating the length and angle of the jth crack, we choose that input flux which yields the largest value of A_j on the jth crack, since as discussed in section 4.2, this should yield the most stable estimates.

As an example we again take Ω as the unit circle, two input fluxes, $g_1(t) = \sin(t)$ and $g_2(t) = \cos(t)$, and five cracks with parameters as listed below:

Crack	Center	θ	L
1	$(-0.4, -0.4)$	0.0	0.2
2	$(-0.06, 0.56)$	0.4	0.3
3	$(0.65, -0.03)$	-0.2	0.3
4	$(-0.73, 0.21)$	1.0	0.25
5	$(0.57, -0.63)$	0.8	0.2

We also reconstruct the cracks with noisy data: we add independent Gaussian error of magnitude 0.001 (about 2 percent of the maximum value of $u - u_0$) to each of the 50 boundary data points.

Below we again plot the first 10 singular values of $\mathbf{M}$, computed from the noisy

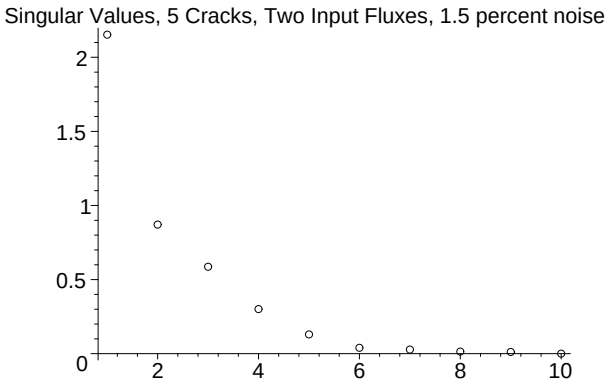

Fig. 3. Singular Values of $\mathbf{M}$, 5 cracks, noisy data.

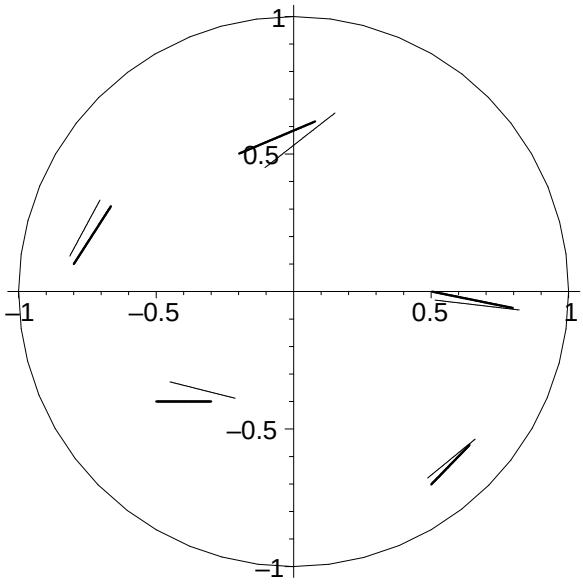

Fig. 4. True and estimated cracks for noisy data, two input fluxes.

data: We again threshold at 5 percent of the maximum singular value, which yields an estimate of five cracks. So far as estimating the number of cracks, the procedure seems relatively robust against reasonable amounts of noise.

Below is a picture of the resulting estimated and true cracks based on the noisy data and using the algorithm outlined above.

To illustrate the advantages of using the optimal input current fluxes, we now use the tentative estimates of the crack locations above to compute the optimal L^2 flux as per section 4.2 for each of the five cracks. We then use all five of the input fluxes to recover the cracks as outlined above (introducing the same level of noise into the measured Dirichlet data). Below is a picture of the resulting estimated and true cracks based on the noisy data using all five optimal L^2 fluxes: This is a reasonable improvement over the previous estimates.

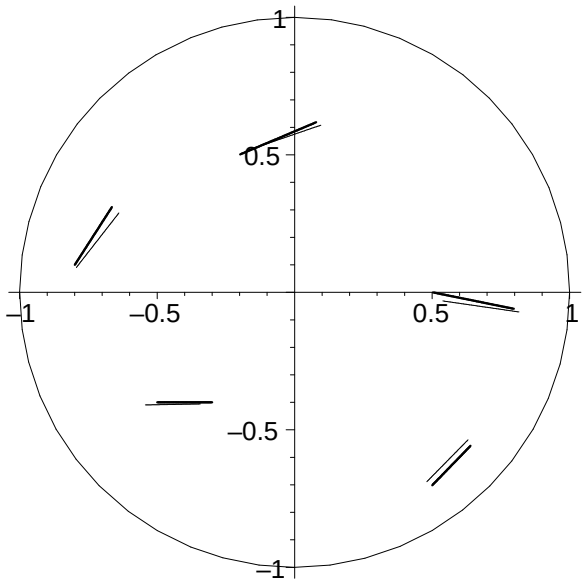

Fig. 5. True and estimated cracks for noisy data, optimal fluxes.

5 Relating Crack Length and Jump Integral

The goal of this section is to prove Lemma 1. In what follows we use u_0 to denote the harmonic function on the "uncracked" domain Ω with Neumann data g and $\int_{\partial\Omega} u_0\, ds = 0$, while u denotes the solution to (1)-(3).

For the moment we assume that Ω contains a single linear crack σ. After translation and rotation we may suppose that Ω contains a neighborhood of the origin and that the crack σ lies inside of Ω on the interval $(0, \epsilon)$ on the x-axis for some $\epsilon > 0$. Let the unit normal vector to σ be given by $\mathbf{n}_\sigma = (0, 1)$. We let $\Gamma(x) = \frac{1}{2\pi}\log(|x|)$ (where $x = (x_1, x_2)$) denote the Green's Function for the Laplacian operator in $\mathbb{R}^2$.

5.1 Formulation as an Integral Equation

We shall first approximate the function u as a perturbation of u_0, in the form $u \approx \tilde{u} := u_0 + v$, where we take $v(x)$ to be of the form

$$v(x) = \int_0^\epsilon \frac{\partial \Gamma}{\partial x_2}(x_1 - t, x_2)\psi(t)\, dt,$$

a double-layer potential based on σ, with suitably chosen density function ψ. Standard potential-theoretic computations show that v is harmonic away from σ, $[v] = \psi$ on σ, and that $\frac{\partial v}{\partial x_2}$ is well-defined and continuous over σ with

$$\lim_{b\to 0} \frac{\partial v}{\partial x_2}(x_1, b) = \frac{1}{2\pi} \text{p.v.} \int_0^\epsilon \frac{\psi'(t)}{t - x_1}\, dt \tag{22}$$

provided ψ is C^2 on σ.

We determine the v by choosing $\psi(s)$ so that $\frac{\partial v}{\partial \mathbf{n}} = -\frac{\partial u_0}{\partial \mathbf{n}}$ on σ, which in light of equation (22) leads to the integral equation

$$\text{p.v.} \int_0^\epsilon \frac{\psi'(t)}{t - x_1}\, dt = -2\pi \frac{\partial u_0}{\partial x_2}(x_1, 0) \tag{23}$$

for $0 < x < \epsilon$. Our goal is to find a suitable function ψ that solves equation (23), and so we will have $\frac{\partial \tilde{u}}{\partial x_2} = 0$ on σ. Note however that $\tilde{u}$ will not have the correct Neumann data on $\partial\Omega$, but as shown below, it will be "close enough."

In what follows we will write σ_ϵ when we need to emphasize the crack's dependence on ϵ. The function u_0 is smooth near σ_ϵ and so we have

$$\begin{aligned} \frac{\partial u_0}{\partial x_2}(x_1, 0) &= \frac{\partial u_0}{\partial x_2}(z^*, 0) + \frac{\partial^2 u_0}{\partial x_1 \partial x_2}(q(x_1), 0)(x_1 - z^*) \\ &= \frac{\partial u_0}{\partial x_2}(z^*, 0) + \epsilon R(x_1) \end{aligned}$$

where $z^* = \epsilon/2$ is the midpoint of σ_ϵ, $q(x_1)$ denotes some number between z^* and x_1, and $R(x_1) = (\frac{x_1 - z^*}{\epsilon}) \frac{\partial^2 u_0}{\partial x_1 \partial x_2}(q(x_1), 0)$. Note that R, as well as its derivative, can be bounded in terms of $\|g\|_{L^2(\partial\Omega)}$.

The solution $\psi(t)$ to equation (23) that we require can be expressed as $\psi(t) = -2\pi \frac{\partial u_0}{\partial x_2}(z^*, 0)\phi(t)$ where ϕ satisfies

$$\text{p.v.} \int_0^\epsilon \frac{\phi'(t)}{t - x_1}\, dt = 1 + \epsilon r(x) \tag{24}$$

with $r(x) = R/(\partial u_0(z^*)/\partial x_2)$, provided that z^* is not a critical point for u_0. The following theorem, although not the strongest possible, is more than sufficient for our purposes.

Lemma 3 *Let $f \in C^3[0,1]$ and $\delta > 0$ a real constant. Then the integral equation*

$$\text{p.v.} \int_0^1 \frac{\phi'(t)}{t-s}\, dt = 1 + \delta f(s), \quad 0 < s < 1, \tag{25}$$

has a unique solution ϕ of the form

$$\phi(t) = -\frac{1}{\pi}\sqrt{t - t^2} + \delta\psi_1(t)$$

which is continuous on $[0,1]$, twice continuously-differentiable on $(0,1)$, with ϕ' integrable on $(0,1)$ and $\phi(0) = \phi(1) = 0$. Also, $\|\psi_1\|_\infty$ is bounded by $\|f\|_{C^3[0,1]}$.

Note that for such a function the principle value integral will exist for each $s \in (0,1)$ since ϕ' is continuously differentiable.

To prove the Lemma we cast equation (25) into an alternate form. We proceed as in section 9.5.2 of [13]: Integrate both sides of equation (25) in s from $s = 0$ to $s = x$ to obtain

$$-\int_0^1 \ln(2|x-t|)\phi'(t)\, dt = x + \delta \int_0^x f(s)\, ds - C_1 \tag{26}$$

for a constant $C_1 = \int_0^1 \ln(2s)\phi'(s)\, ds$, where the legitimacy of the integration and swapping of order is justified by equation (9.12) and Lemma 9.1 in [13], and the constant C_1 may be considered arbitrary. Any solution to equation (25) with the stated regularity satisfies equation (26). Conversely, as shown in that text (again, section 9.5.2) any solution to (26) also satisfies (25).

Now integrate by parts on the left in equation (26) to transfer the derivative off of ϕ, taking care to interpret the resulting principal value terms correctly (briefly, split the integral into pieces over intervals $(0, x-\epsilon)$ and $(x+\epsilon, 1)$, integrate by parts on each, then take the limit as $\epsilon \to 0$) and use $\phi(0) = \phi(1) = 0$ to obtain

$$\text{p.v.} \int_0^1 \frac{\phi(t)}{t-x}\, dt = x + \delta F(x) - C_1 \tag{27}$$

where $F(x) = \int_0^x f(s)\, ds$. Any solution to equation (27) necessarily satisfies equation (26), provided ϕ has the required regularity.

Again employ the technique which lead to equation (26), integrate both sides of equation (27) in x from $x = 0$ to $x = y$ to obtain

$$-\int_0^1 \ln(2|y-t|)\phi(t)\,dt = \frac{1}{2}y^2 + \delta\int_0^y F(t)\,dt - C_1 y + C_2 \tag{28}$$

in which C_2 may be considered a second arbitrary constant at our disposal. The same reasoning which showed the equivalence of equations (25) and (26) also shows the equivalence of equations (27) and (28). We will show that equation (28), and hence equation (25), possesses a unique solution with the required regularity and $\phi(0) = \phi(1) = 0$.

As in [13] we make the (invertible) substitution $y = \cos^2(\sigma/2)$, $t = \cos^2(\theta/2)$ in equation (28) and obtain

$$-\int_0^\pi \ln|\cos(\theta) - \cos(\sigma)|\hat{\phi}(\theta)\,d\theta = g(\sigma) \tag{29}$$

for $0 < \sigma < \pi$, where $\hat{\phi}(\theta) = \frac{1}{2}\phi(\cos^2(\theta/2))\sin(\theta)$ and

$$g(\sigma) = C_2 - C_1\cos^2(\sigma/2) + \frac{1}{2}\cos^4(\sigma/2) + \frac{\delta}{2}\int_\sigma^\pi F(\cos^2(\theta/2))\sin(\theta)\,d\theta.$$

By using $\cos^2(\sigma/2) = (1+\cos(\sigma))/2$ we obtain

$$\begin{aligned} g(\sigma) = &\left(C_2 - \frac{C_1}{2} + \frac{3}{16}\right) + \left(-\frac{C_1}{2} + \frac{1}{4}\right)\cos(\sigma) \\ &+ \frac{1}{16}\cos(2\sigma) + \frac{\delta}{2}\int_\sigma^\pi F(\cos^2(\theta/2))\sin(\theta)\,d\theta. \end{aligned}$$

Equation (29) can thus be written

$$(K\hat{\phi})(\sigma) = g(\sigma) \tag{30}$$

where K denotes the integral operator on the left side of equation (29), $g(\sigma) \equiv c_1 + c_2\cos(\sigma) + \frac{1}{16}\cos(2\sigma) + \delta G(\sigma)$ with $c_1 = -C_1/2 + C_2 + 3/16$, $c_2 = -C_1/2 + 1/4$, and

$$G(\sigma) = \frac{1}{2}\int_\sigma^\pi F((1+\cos(\theta))/2)\sin(\theta)\,d\theta. \tag{31}$$

We will show that for any given choice of C_1 and C_2 equation (30) possesses a unique solution in $L^2(0,\pi)$, and that this solution can be used to recover the solution to equation (25).

To see this, note that the operator K is compact and self-adjoint on $L^2(0,\pi)$, with eigenvalues $\mu_0 = \pi\ln(2)$, $\mu_n = \pi/n$ for $n \geq 1$, and orthonormal eigenfunctions $\phi_0(\sigma) = 1/\sqrt{\pi}$, $\phi_n(\sigma) = \sqrt{2/\pi}\cos(n\sigma)$ for $n \geq 1$ (see [13], section 9.5.2). The unique $L^2(0,\pi)$ solution to equation (30) is thus given by

$$\begin{aligned}\hat{\phi}(\sigma) &= \sum_{n=0}^{\infty} \frac{1}{\mu_n}(g,\phi_n) \\ &= \sum_{n=0}^{\infty} \frac{1}{\mu_n}(c_1 + c_2\cos(\sigma) + \frac{1}{16}\cos(2\sigma),\phi_n)\phi_n + \delta\sum_{n=0}^{\infty}\frac{1}{\mu_n}(G,\phi_n)\phi_n \\ &= \frac{c_1}{\pi\ln(2)} + \frac{c_2}{\pi}\cos(\sigma) + \frac{1}{8\pi}\cos(2\sigma) + \delta\sum_{n=0}^{\infty}\frac{1}{\mu_n}(G,\phi_n)\phi_n \qquad (32)\end{aligned}$$

where $(\cdot,\cdot)$ denotes the L^2 inner product, provided the last sum on the right in (32) converges in $L^2(0,\pi)$. This requires

$$\sum_{n=1}^{\infty}(\frac{1}{\mu_n}(G,\phi_n))^2 < \infty. \qquad (33)$$

We now show that this is true, and that in fact the sum on the right in (32) actually represents a $C^2(0,\pi)$ function. With G as defined by equation (31) repeated integration by parts (taking derivatives off of $\sin(n\sigma)$ or $\cos(n\sigma)$, putting derivatives on G) shows that

$$\int_0^{\pi} G(\sigma)\cos(n\sigma)\,d\sigma = -\frac{1}{n^5}\int_0^{\pi}\sin(n\sigma)G^{(5)}(\sigma)\,d\sigma$$

since all endpoint terms at $\sigma = 0$ and $\sigma = \pi$ in each integration by parts fortuitously vanish. The function $G^{(5)}$ (which involves derivatives of f up the third order) is in $L^2(0,\pi)$, so that we find $\frac{1}{\mu_n}(G,\phi_n) = \frac{d_n}{n^4}$ with $d_n = -\sqrt{2/\pi^3}(G^{(5)},\sin(n\sigma))$, and so $\sum_n d_n^2 < \infty$. As a result the sum

$$\sum_{n=1}^{\infty}\frac{1}{\mu_n}(G,\phi_n)\phi_n(\sigma) = \sqrt{2/\pi}\sum_{n=1}^{\infty}\frac{d_n}{n^4}\cos(n\sigma)$$

is in $L^2(0,\pi)$, and term-by-term differentiation shows the sum possesses a third derivative in $L^2(0,\pi)$, and hence a continuous second derivative on $[0,\pi]$. Thus the unique (for a given choice of C_1 and C_2) $L^2(0,\pi)$ solution $\hat{\phi}(\sigma)$ to equation

(29) is given by

$$\hat{\phi}(\sigma) = \frac{c_1}{\pi \ln(2)} + \frac{c_2}{\pi}\cos(\sigma) + \frac{1}{8\pi}\cos(2\sigma) + \delta H(\sigma)$$

where

$$H(\sigma) = d_0 + \sum_{n=1}^{\infty} \frac{d_n}{n^4}\cos(n\sigma)$$

for the square-summable sequence $\{d_n\}$.

Note that if a $C[0,1]$ solution $\phi(y)$ to equation (25) exists, the corresponding function $\hat{\phi}$ satisfying equation (30) will certainly be in $L^2(0,\pi)$. Thus by considering equation (30), we can be sure to locate a $C[0,1]$ to equation (25) if it exists.

Use $\sigma = 2\arccos(\sqrt{y})$ to obtain

$$\hat{\phi}(\sigma) = \frac{c_1}{\pi \ln(2)} + \frac{c_2}{\pi}\cos(2\arccos(\sqrt{y})) + \frac{1}{8\pi}\cos(4\arccos(\sqrt{y})) + \delta H(2\arccos(\sqrt{y})).$$

Note that $\cos(2\arccos(\sqrt{y})) = 2y - 1$ and $\cos(4\arccos(\sqrt{y})) = 8y^2 - 8y + 1$ for $0 < y < 1$. With $y = \cos^2(\sigma/2)$ and $\hat{\phi}(\sigma) = \frac{1}{2}\phi(\cos^2(\sigma/2))\sin(\sigma)$ we have $\sin(\sigma) = 2\sqrt{y - y^2}$ so that

$$\phi(y) = \frac{\alpha(y)}{\sqrt{y - y^2}}$$

where

$$\alpha(y) = \frac{c_1}{\pi \ln(2)} + \frac{c_2}{\pi}(2y - 1) + \frac{1}{8\pi}(8y^2 - 8y + 1) + \delta\tilde{H}(y)$$

with $\tilde{H}(y) = H(2\arccos(\sqrt{y}))$. Also note that

$$\tilde{H}(y) = d_0 + \sum_{n=1}^{\infty} \frac{d_n}{n^4}\cos(2n\arccos(\sqrt{y})) = d_0 + \sum_{n=1}^{\infty} \frac{d_n}{n^4} T_n(2y - 1) \tag{34}$$

where T_n denotes the nth Chebyshev polynomial of the first kind, which can be defined by $T_n(x) = \cos(2n\arccos(\sqrt{(x+1)/2}))$ (easily derived from the well-known formula $T_n(x) = \cos(n\arccos(x))$ and the half-angle formula). Although $\hat{\phi}$ is in $L^2(0,\pi)$, this does not guarantee that $\phi(y)$ lies in $L^2(0,1)$. However, the latter is indeed guaranteed if the constants c_1 and c_2 (or equivalently, C_1 and C_2) are chosen correctly, as shown below.

Before proceeding, note that the Chebyshev polynomials satisfy the conditions $\sup_{-1\le x\le 1}|T_n(x)| = 1$ and $\sup_{-1\le x\le 1}|T_n'(x)| = n^2$. Moreover, since

$d_k = -\sqrt{2/\pi^3}(G^{(5)}, \sin(k\sigma))$ and $G^{(5)}$ can be bounded in terms of $\|f\|_{C^3}$, we have $|d_k| \le C\|f\|_{C^3}$ for some constant C and all k. From (34) it is thus clear that $\tilde{H}(y)$ is continuous on $[0,1]$, and term-by-term differentiation of the right side of (34) shows that $\tilde{H}'(y)$ is also continuous on $[0,1]$. In particular, $\tilde{H}(y)$ is in $C^1[0,1]$, and hence so is $\alpha(y)$. Finally, note that

$$|\tilde{H}(y)| = \left| d_0 + \sum_{n=1}^{\infty} \frac{d_n}{n^4} T_n(2y-1) \right| \le \sup_n |d_n| \sum_{n=1}^{\infty} \frac{1}{n^4} \le C\|f\|_{C^3}. \tag{35}$$

and similarly

$$|\tilde{H}'(y)| = \left| \sum_{n=1}^{\infty} \frac{2d_n}{n^4} T_n'(2y-1) \right| \le 2 \sup_n |d_n| \sum_{n=1}^{\infty} \frac{1}{n^2} \le C\|f\|_{C^3} \tag{36}$$

for $0 < y < 1$.

If we choose C_1 and C_2 in equation (28) as

$$\begin{aligned} C_1 &= \frac{1}{2} + \delta\pi(\tilde{H}(1) - \tilde{H}(0)) \\ C_2 &= \frac{1 - 2\ln(2)}{16} + \frac{\delta\pi}{2}(\tilde{H}(1) - \tilde{H}(0)) - \frac{\delta\pi \ln(2)}{2}(\tilde{H}(0) + \tilde{H}(1)) \end{aligned}$$

then $\alpha(0) = \alpha(1) = 0$ and we find that ϕ is continuous on $[0,1]$ with $\lim_{y\to 0^+} \phi(y) = \lim_{y\to 1^-} \phi(y) = 0$, and in fact

$$\phi(y) = -\frac{1}{\pi}\sqrt{y - y^2} + \delta\psi_1(y) \tag{37}$$

with

$$\psi_1(y) = \frac{(\tilde{H}(0) - \tilde{H}(1))y - \tilde{H}(0) + \tilde{H}(y)}{\sqrt{y - y^2}} \tag{38}$$

To verify the remaining properties of ϕ, let $r(y) = (\tilde{H}(0) - \tilde{H}(1))y - \tilde{H}(0) + \tilde{H}(y)$ so that $r(0) = 0$ and

$$r'(y) = \tilde{H}(0) - \tilde{H}(1) + \tilde{H}'(y).$$

From this and estimates (35), (36), we have

$$r(y) = \int_0^y r'(x)\,dx \le C\|f\|_{C^3} y.$$

One can similarly obtain a bound $r(y) \leq C\|f\|_{C^3}(1-y)$, so that in fact $r(y) \leq C\|f\|_{C^3}(y-y^2)$ for $0 < y < 1$. Combining this with (38) provides a bound $\psi_1(y) \leq C\|f\|_{C^3}\sqrt{y-y^2}$, and in particular shows that ϕ is continuous on $[0,1]$. Clearly $\|\psi_1\|_\infty \leq C\|f\|_{C^3}$. The estimate on $r(y)$ also makes it simple to check that $\phi'(y)$ is integrable on $(0,1)$ which completes the proof of Lemma 3. $\Box$.

Remark: A simple change of variables in the integral equation of Lemma 3 shows that the integral equation

$$\text{p.v.} \int_{-\epsilon/2}^{\epsilon/2} \frac{\phi'(t)}{t-s}\, dt = 1 + \delta f(s), \quad -\epsilon/2 < s < \epsilon/2, \tag{39}$$

has a unique solution ϕ of the form

$$\phi(t) = -\frac{1}{\pi}\sqrt{\epsilon^2/4 - t^2} + \delta\epsilon\psi_1(t)$$

which is continuous on $[-\epsilon/2, \epsilon/2]$, twice continuously-differentiable on $(-\epsilon/2, \epsilon/2)$, with ϕ' integrable on $(-\epsilon/2, \epsilon/2)$ and $\phi(-\epsilon/2) = \phi(\epsilon/2) = 0$. Also, $\|\psi_1\|_\infty$ is bounded by $\|f\|_{C^3[-\epsilon/2,\epsilon/2]}$.

5.2 Proof of Lemma 1

The following Lemma will be useful.

Lemma 4 *Let Ω be a bounded region in $\mathbb{R}^2$ and $\Sigma = \cup_{j=1}^n \sigma_j$, with each σ_j a line segment with center $z_j^* \in \Omega$, at angle θ_j and with length ϵL_j. Let $\phi \in H^1(\Omega \setminus \Sigma)$ satisfy $\triangle\phi = 0$ in $\Omega \setminus \Sigma$ with $\frac{\partial\phi}{\partial \mathbf{n}} = h_0$ on $\partial\Omega$, $\frac{\partial\phi}{\partial \mathbf{n}} = h_j$ on σ_j and continuous across σ_j, with $h_0 \in L^2(\partial\Omega)$ and $h_j \in L^2(\sigma_j)$. Assume ϕ has been normalized so that $\int_{\partial\Omega} \phi\, ds = 0$. Then*

$$\|\phi\|_{H^1(\Omega\setminus\Sigma)} \leq C(\|h_0\|_{L^2(\partial\Omega)} + \sum_{j=1}^n \|h_j\|_{L^2(\sigma_j)})$$

where C is independent of $\epsilon > 0$ for all sufficiently small ϵ.

Proof: The proof is really quite standard—the only twist is the independence of C from ϵ. In what follows we will use the notation Σ_ϵ when we need to emphasize the dependence of Σ on the scale parameter ϵ.

An application of the divergence theorem shows that

$$\int_{\Omega\setminus\Sigma} |\nabla\phi|^2\,dx = \int_{\partial\Omega} \phi h_0\,ds - \sum_{j=1}^{n}\int_{\sigma_j}[\phi]h_j\,ds$$

from which we obtain

$$\|\nabla\phi\|_{L^2(\Omega\setminus\Sigma)} \le \|\phi\|_{L^2(\partial\Omega)}\|h_0\|_{L^2(\partial\Omega)} + \sum_{j=1}^{n}\|[\phi]\|_{L^2(\sigma_j)}\|h_j\|_{L^2(\sigma_j)}. \tag{40}$$

We also have, from standard trace estimates, $\|\phi\|_{L^2(\partial\Omega)} \le C\|\phi\|_{H^1(\Omega\setminus\Sigma)}$ and $\|[\phi]\|_{L^2(\sigma_j)} \le C\|\phi\|_{H^1(\Omega\setminus\Sigma)}$, where in the latter case we can clearly take C independent of ϵ for all sufficiently small $\epsilon > 0$ (since the crack σ_j^1 of length $\epsilon_1 L_j$ is contained in the crack σ_j^2 of length $\epsilon_2 L_j$ for $\epsilon_1 < \epsilon_2$, for fixed z_j^* and θ_j). From equation (40) we may then conclude that

$$\|\nabla\phi\|_{L^2(\Omega\setminus\Sigma)} \le C\|\phi\|_{H^1(\Omega\setminus\Sigma)}\left(\|h_0\|_{L^2(\partial\Omega)} + \sum_{j=1}^{n}\|h_j\|_{L^2(\sigma_j)}\right) \tag{41}$$

with C independent of ϵ, and all h_j.

Finally, we use the Poincaré inequality

$$\|\phi\|_{L^2(\Omega\setminus\Sigma)} \le C_2\|\nabla\phi\|_{L^2(\Omega\setminus\Sigma)} \tag{42}$$

(making use of $\int_{\partial\Omega}\phi\,ds = 0$) where C_2 can be taken independent of $\epsilon > 0$ for sufficiently small ϵ. To prove that C_2 in the estimate (42) can indeed be taken independently of ϵ, note that the smallest eigenvalue for the Laplacian with boundary conditions $\frac{\partial\phi}{\partial\mathbf{n}} = 0$ on the space $V(\epsilon) = \{\phi \in H^1(\Omega\setminus\Sigma_\epsilon), \int_{\partial\Omega}\phi\,ds = 0\}$ is given by

$$\lambda_\epsilon = \inf_{V(\epsilon)} \frac{\|\nabla\phi\|_{L^2(\Omega\setminus\Sigma_\epsilon)}}{\|\phi\|_{L^2(\Omega\setminus\Sigma_\epsilon)}} = \inf_{V(\epsilon)} \frac{\|\nabla\phi\|_{L^2(\Omega)}}{\|\phi\|_{L^2(\Omega)}}$$

where we interpret the integrals over Ω by extending $\nabla\phi$ or ϕ by zero to all of Ω. Since $V(\epsilon_1) \subset V(\epsilon_2)$ for $\epsilon_1 < \epsilon_2$, we clearly have $\lambda_{\epsilon_1} \ge \lambda_{\epsilon_2}$ for $\epsilon_1 < \epsilon_2$. Fix $\epsilon_0 > 0$ so that $\Sigma_{\epsilon_0} \subset \Omega$ and so for all $\epsilon < \epsilon_0$ we have $\lambda_\epsilon \ge \lambda_{\epsilon_0}$. It then follows that for $\phi \in V(\epsilon)$ we have

$$\frac{\|\nabla\phi\|_{L^2(\Omega\setminus\Sigma_\epsilon)}}{\|\phi\|_{L^2(\Omega\setminus\Sigma_\epsilon)}} \ge \lambda_\epsilon \ge \lambda_{\epsilon_0}.$$

A bit of rearrangement gives

$$\|\phi\|_{L^2(\Omega\setminus\Sigma_\epsilon)} \le \frac{1}{\lambda_{\epsilon_0}}\|\nabla\phi\|_{L^2(\Omega\setminus\Sigma_\epsilon)}$$

which shows inequality (42).

Combining equations (41) and (42) proves Lemma 4. □.

Note that standard trace estimates also yield

$$\|\phi\|_{L^2(\partial\Omega)} \leq C(\|h_0\|_{L^2(\partial\Omega)} + \sum_{j=1}^{n} \|h_j\|_{L^2(\sigma_j)}) \tag{43}$$

with C independent of ϵ.

To prove Lemma 1, consider any single crack $\sigma \in \Sigma$ with center z^*, length ϵL, and angle θ. After translation and rotation we may assume that z^* is the origin and that the crack σ spans the interval $(-\epsilon L/2, \epsilon L/2)$ along the x_1 axis. Note that on the crack $\frac{\partial}{\partial \mathbf{n}} = \frac{\partial}{\partial x_2}$.

Let a function v be defined as

$$v(x) = \int_{-\epsilon L/2}^{\epsilon L/2} \frac{\partial \Gamma}{\partial x_2}(x_1 - t, x_2)\phi(t)\, dt \tag{44}$$

with ϕ chosen so that $\frac{\partial v}{\partial x_2} = -\frac{\partial u_0}{\partial x_2}$ and $\phi(-\epsilon L/2) = \phi(\epsilon L/2) = 0$. Application of Lemma 3 and equation (39) show that ϕ is uniquely determined and is continuous on $[-\epsilon L/2, \epsilon L/2]$, twice-continuously differentiable on $(-\epsilon L/2, \epsilon L/2)$, of the form

$$\phi(s) = 2\frac{\partial u_0}{\partial x_2}(z^*)\sqrt{\epsilon^2 L^2/4 - s^2} + \epsilon^2 \psi_1(s)$$

for some function ψ_1. Note that although ψ_1 depends on ϵ, $\|\psi_1\|_{L^\infty(-\epsilon L/2, \epsilon L/2)}$ is bounded for ϵ in any neighborhood of zero.

From the definition of v in equation (44) we have, for any point $x = (x_1, x_2)$ at a distance d from σ,

$$\frac{\partial v}{\partial x_1}(x) = \frac{1}{\pi} \int_{-\epsilon L/2}^{\epsilon L/2} \frac{(x_1 - s)x_2}{((x_1 - s)^2 + x_2^2)^2}\phi(s)\, ds$$

$$\frac{\partial v}{\partial x_2}(x) = -\frac{1}{2\pi} \int_{-\epsilon L/2}^{\epsilon L/2} \frac{(x_1 - s)^2 - x_2^2}{((x_1 - s)^2 + x_2^2)^2}\phi(s)\, ds$$

We can then bound the magnitude of $\nabla v(x)$ as

$$
\begin{aligned}
|\nabla v(x)| &= \left(\left(\frac{\partial v}{\partial x_1} \right)^2 + \left(\frac{\partial v}{\partial x_2} \right)^2 \right)^{1/2} \\
&\leq \left(\frac{1}{4\pi^2} \int_{-\epsilon L/2}^{\epsilon L/2} \frac{1}{((x_1 - s)^2 + x_2^2)^2} \, ds \right)^{1/2} \left(\int_{-\epsilon L/2}^{\epsilon L/2} \phi^2(s) \, ds \right)^{1/2} \\
&\leq C \frac{\sqrt{\epsilon}}{d^2} \sqrt{\epsilon^3/6} \\
&\leq \frac{\tilde{C}}{d^2} \epsilon^2
\end{aligned} \tag{45}
$$

for some constant $\tilde{C}$ independent of ϵ.

More generally, consider the case of n cracks, $\Sigma = \cup_{j=1}^n \sigma_j$, with centers z_j, lengths ϵL_j. For each crack define

$$
v_j(x) = \int_{\sigma_j} \frac{\partial \Gamma}{\partial \mathbf{n}_x}(x - y) \phi_j(y) \, ds_y
$$

with $\phi_j(y)$ chosen so that $\frac{\partial v_j}{\partial \mathbf{n}} = -\frac{\partial u_0}{\partial \mathbf{n}}$ on σ_j. From the preceding analysis, each $\phi_j(y)$ is of the form

$$
\phi_j(y(s)) = 2 \frac{\partial u_0}{\partial \mathbf{n}}(z_j^*) \sqrt{\epsilon^2 L_j^2/4 - s^2} + \epsilon^2 \psi_j(s) \tag{46}
$$

where $s \in (-\epsilon L_j/2, \epsilon L_j/2)$ indexes position along the crack and ψ_j is bounded. Recall also that $[v_j] = \phi_j$ on σ_j. From equation (45) we find that

$$
|\nabla v_j(x)| \leq C \frac{\epsilon^2}{|x - \sigma_j|^2} \tag{47}
$$

where $|x - \sigma_j|$ denotes the distance from x to σ_j; the constant C can be taken independently of the crack.

Consider the approximation to u given by $\tilde{u}_1 := u_0 + v$ with

$$
v = \sum_{j=1}^n v_j. \tag{48}
$$

The function v (and hence $\tilde{u}_1$) is harmonic on $\Omega \setminus \Sigma$. Also note that $\frac{\partial \tilde{u}_1}{\partial \mathbf{n}}$ is continuous across each crack and smooth along the crack. Since $\frac{\partial u_0}{\partial \mathbf{n}} = g$ on

$\partial\Omega$, and in light of the bound (47), we have

$$\left\| \frac{\partial \tilde{u}_1}{\partial \mathbf{n}} - g \right\|_{L^2(\partial\Omega)} \leq C\epsilon^2$$

for some constant C, which may depend on the crack centers, angles, and the L_j, but not the common scale ϵ. Moreover, since the crack centers z_j^* are distinct we have from (45) that for all ϵ in some neighborhood of zero

$$\left\| \frac{\partial \tilde{u}_1}{\partial \mathbf{n}} \right\|_{L^2(\sigma_j)} \leq C\epsilon^{5/2}$$

on each crack (using the fact that $|\sigma_j| = O(\epsilon)$).

Construct a refined approximation $\tilde{u}_2$ as $\tilde{u}_2 = \tilde{u}_1 + w = u_0 + v + w$ where w is harmonic on Ω with $\frac{\partial w}{\partial \mathbf{n}} = -\frac{\partial \tilde{u}_1}{\partial \mathbf{n}}$ on $\partial\Omega$. Standard estimates (e.g., Lemma 4 with Σ empty) show that $\|\frac{\partial w}{\partial \mathbf{n}}\|_{L^2(\sigma_j)} \leq C\epsilon^{5/2}$. Let $\phi = u - \tilde{u}_2$. We then have $\triangle\phi = 0$ in $\Omega \setminus \Sigma$ with $\frac{\partial \phi}{\partial \mathbf{n}} = 0$ on $\partial\Omega$ and $\|\frac{\partial \phi}{\partial \mathbf{n}}\|_{L^2(\sigma_j)} \leq C\epsilon^{5/2}$. Application of Lemma 4 shows that $\|\phi\|_{H^1(\Omega\setminus\Sigma_\epsilon)} \leq C\epsilon^{5/2}$ with C independent of ϵ. From this we deduce that $\|[\phi]\|_{L^2(\sigma_j)} \leq C\epsilon^{5/2}$ where as above, we may take C independent of ϵ as per the remarks after equation (40).

We then have

$$\left| \int_{\sigma_j} [\phi]\, ds \right| \leq \int_{\sigma_j} |[\phi]|\, ds \leq |\sigma_j|^{1/2} \|[\phi]\|_{L^2(\sigma_j)} \leq C\epsilon^3$$

the last step via Hölder's inequality. Note also that on any crack we have $[\phi] = [u] - [u_0] - [v] - [w] = [u] - [v]$ since u_0 and w are harmonic on Ω. As a result we have, on each crack σ_j,

$$\left| \int_{\sigma_j} [\phi]\, ds \right| = \left| \int_{\sigma_j} [u]\, ds - \int_{\sigma_j} [v]\, ds \right| \leq C\epsilon^3. \tag{49}$$

From equation (46) we have $[v](s) = \phi_j(y(s)) = 2\frac{\partial u_0}{\partial \mathbf{n}}(z_j^*)\sqrt{\epsilon^2 L_j^2/4 - s^2} + \epsilon^2\psi_j(s)$ on σ_j so that

$$\begin{aligned} \int_{\sigma_j} [v](s)\, ds &= \int_{-L\epsilon/2}^{L\epsilon/2} \left(2\frac{\partial u_0}{\partial \mathbf{n}}(z_j^*)\sqrt{\epsilon^2 L_j^2/4 - s^2} + \epsilon^2\psi_j(s) \right) ds \\ &= \frac{\pi}{4}\epsilon^2 L_j^2 \frac{\partial u_0}{\partial \mathbf{n}}(z_j^*) + O(\epsilon^3) \end{aligned} \tag{50}$$

Combining equations (49) and (50) proves Lemma 1.

References

[1] Alessandrini, F., and Diaz Valenzuela, A., Unique determination of multiple cracks by two measurements, Siam J Cont Opt, 34 (3), 1996, pp. 913-921.

[2] Ammari, H., Moskow, S., and Vogelius, M., Boundary integral formulae for the reconstruction of electric and electromagnetic inhomogeneities of small volume. ESAIM: Cont. Opt. Calc. Var., 9 (2003), pp. 49–66.

[3] Andersen, K., Brooks, S., and Hansen, M., A Bayesian approach to crack detection in electrically conducting media, Inverse Problems, **17**, 2001, pp. 121-136.

[4] Andrieux, S., Ben Abda, A., and Bui, H.D., Reciprocity principle and crack identification, Inverse Probl, 15 (1), 1999, pp. 59-65.

[5] Andrieux, S., and Ben Abda, A., Identification de fissures planes par une donne de bord unique; un procd direct de localisation et didentification, C.R. Acad. Sci., Paris I, 1992, 315, pp. 1323-1328.

[6] Bryan, K., Vogelius, M., A uniqueness result concerning the identification of a collection of cracks from finitely many electrostatic boundary measurements, Siam J. Math. 6, 1992, pp 950-958.

[7] Bryan, K., Liepa, V., and Vogelius, M., Reconstruction of multiple cracks from experimental electrostatic boundary measurements, Inverse Problems and Optimal Design in Industry, 7, 1993, pp. 147-167.

[8] Bryan, K., Vogelius, M., A review of selected works on crack identification, in "Geometric Methods in Inverse Problems and PDE Control", IMA Volume 137, Springer-Verlag, 2004.

[9] Friedman, A., and Vogelius, M., *Determining cracks by boundary measurements*, Ind U Math J, **38**, 1989, pp. 527-556.

[10] Kim, H., and Seo, J., Unique determination of a collection of a finite number of cracks from two boundary measurements, Siam J. Math. Anal. **27**, 1996, pp. 1336-1340.

[11] Liepa, V., Santosa, F., and Vogelius, M., *Crack determination from boundary measurements—reconstruction using experimental data*, J. Nondestructive Evaluation, **12**, 1993, pp.163-174.

[12] Osborne, M.R., and Smyth, G.K., A modified prony algorithm for exponential function fitting, SIAM J. Sci. Comp., 16, 1995, pp 119-138.

[13] Porter, D. and Stirling, D., Integral Equations: a practical treatment, from spectral theory to applications.

[14] Santosa, F., and Vogelius, M., *A computational algorithm to determine cracks from electrostatic boundary measurements*, Int J Engr Sci, **29**, 1991, pp. 917-937.